Numerical Analysis of Response of Geocell Confined Flexible Pavement

Ram Babu[1] and G. L Sivakumar Babu[2]
[1,2]*Department of Civil Engineering, Indian Institute of Science, Bangalore, India*
E-mail: gls@civil.iisc.ernet.in

ABSTRACT: Geocell is one of the recent forms of reinforcing material that is increasingly used in applications in flexible pavements. In the present work, the benefit provided by geocell- reinforcement to the flexible pavement in terms of settlement as well as fatigue and rutting strains reductions are analysed. A simple composite model for geocell-reinforced soil is proposed to represent the three dimensional structure. To investigate the behaviour of geocell reinforcement in the flexible pavement, a series of numerical analyses are carried out to understand the effect of secant modulus of geocell material, aspect ratio, thickness of geocell-reinforced layer, and type of subgrade material and the results are presented in this paper. The results of the analysis are useful in development of guidelines for the design of flexible pavements in using geocells.

KEYWORDS: Geocell reinforcement, Composite model, Flexible pavements, Parametric study

1. INTRODUCTION

In general, in many countries, low volume roads and access roads to various resource industries lead to significant economic development. In some places in South East Asia and India, typically the subgrades of these types of roads are soft to medium dense silty and clayey soils. Construction of unpaved road section with poor subgrade CBR values is very difficult and leads to insufficient structural stability. The structural strength can be improved by geosynthetic and geocell reinforcements. Geosynthetic reinforcement is an established technique of subgrade improvement and base reinforcement for over 40 years. Geocells are three-dimensional honeycombed cellular structures and provide confinement to compacted infill soil. Their confinement reduces the lateral movement of the soil particles and forms a stiffened mattress or slab to distribute applied loads over a wider area.

Development of geocell began with the U.S. Army Corps of Engineers in 1970s to confine the cohesionless soil for the construction of tactical bridge approach roads over soft ground (Webster and Watkins, 1977). Considerable work was carried out to understand the behaviour of geocell reinforced soil during the last three decades. These works were based on experiments and numerical simulations; and a few of them are by Mitchell et al. (1979), Bush et al. (1990), Bathurst and Karpurapu (1993), Cowland and Wong (1993), Rajagopal et al. (1999), Madhavi Latha et al.(2009), Han et.al (2008), Sanat et al. (2010) and Yang et al.(2010). These studies on geocell are based on results from triaxial compression tests, direct shear test, plate load tests, laboratory model tests, and field tests. Most of the published research focused on planar reinforcement and has resulted in several design methods for geotextile or geogrid-reinforced unpaved roads. Only limited research has been done to develop design methods for the geocell reinforcement. Yang (2010) proposed a mechanistic-empirical design model for geocell-reinforced unpaved roads if subgrade and bases are stable. Pokharel (2010) obtained a simplified design method for geocell-reinforced unpaved roads if subgrade is unstable. Sivakumar Babu and Pawan kumar (2012) proposed a design procedure for geocell reinforced flexible pavement sections considering the equivalent elastic modulus concept for geocell composite layers.

A conventional flexible pavement system consists of three layers namely asphalt concrete (AC), granular base course (base), and subgrade layer as shown in Figure 1. AC is the top most layer and the subgrade is the existing compacted strata in the flexible pavement system. The selection of the type, properties and thickness of the base and AC layer is based on the properties of subgrade and traffic loading condition.

The main failure criteria for the design of flexible pavement are fatigue cracking in AC layer and rutting in the subgrade layer as well as surface settlement mainly due to base and subgrade layer.

The critical parameters responsible for these modes of failure are tensile strain below the AC layer and compressive strain above the subgrade layer just below the centreline of load as shown in Figure 1 for fatigue and rutting respectively.

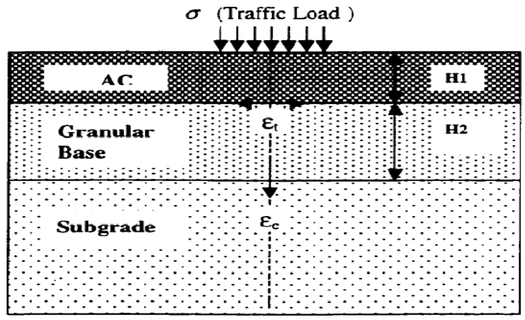

Figure 1 Different layers of flexible pavement

Indian Roads Congress (IRC) adopts mechanistic empirical pavement design procedures presented in IRC: 37-2001. Fatigue criterion is defined in terms of number of cumulative load repetitions and maximum tensile strain generated below AC layer to keep the fatigue cracking within permissible limit. It is also defined in terms of number of cumulative standard axle to produce 20% cracked surface area. Rutting is defined in terms of the number of cumulative standard axle to produce rutting of 20mm. ε_t is maximum tensile strain at the bottom of the AC layer; ε_c is vertical subgrade strain and H1 & H2 are thickness of AC layer & base layer respectively. In this study, it is proposed to examine the effect of geocell in influencing the fatigue and rutting strains as well as surface displacements.

2. PARAMETERS FOR GEOCELL CONFINED SOIL

2.1 Young's modulus for geocell confined soil

The Young's modulus for soil in the absence of geocell is given by

$$E_u = \frac{3(1-2\upsilon)(1+e_0)}{\kappa} p \tag{1a}$$

E_u is the elastic modulus of unreinforced soil; κ is the recompression index of the soil, ν is the poisson's ratio, e_0 is the initial void ratio and p is the mean effective stress.

As per the hoop tension theory, there is an extra confining stress get generated in the presence of geocell. This increment is given as

$$\Delta\sigma_3 = \frac{2M}{D}\left(\frac{1-\sqrt{1-\varepsilon}}{1-\varepsilon}\right) \tag{1b}$$

On inclusion of the extra confining stress the Young's modulus for geocell confined soil layer is derived in the following steps

$$E_g = \frac{3(1-2\upsilon)(1+e_0)}{K}\left(\frac{\sigma_1+2(\sigma_3+\Delta\sigma_3)}{3}\right) \quad (1c)$$

$$E_g = \frac{3(1-2\upsilon)(1+e_0)}{K}\left(\frac{\sigma_1+2\sigma_3}{3}+\frac{2}{3}\Delta\sigma_3\right) \quad (1d)$$

$$E_g = \frac{3(1-2\upsilon)(1+e_0)}{K}\left(p+\frac{2}{3}\Delta\sigma_3\right) \quad (1e)$$

$$E_g = \frac{3(1-2\upsilon)(1+e_0)}{K}p\left(1+\frac{2}{3}\frac{\Delta\sigma_3}{p}\right) \quad (1f)$$

So the Young's modulus for geocell confined soil layer is obtained as

$$E_g = E_u\left(1+\frac{2}{3}\frac{\Delta\sigma_3}{p}\right) \quad (2)$$

$$E_g = E_u\left(1+\frac{4}{3}\frac{M}{pD}\left(\frac{1-\sqrt{1-\varepsilon}}{1-\varepsilon}\right)\right) \quad (3)$$

Above equation is the general expression for the Young's modulus of geocell reinforced soil layer given as E_g, M is the secant modulus of the geocell at an axial strain, ε.

Assuming axial strain generated in geocell is 2.5%. So the above expression becomes

$$E_g = E_u\left(1+\frac{1}{58}\frac{M'}{pD}\right) \quad (4)$$

Here M' is the secant modulus of the geocell at 2.5% axial strain; D is the initial diameter of geocell.

2.2 Shear strength parameters for geocell confined soil

The extra cohesion induced in the soil is related to the increase in confining stress due to the presence of geocell, this is given by Bathurst and Karpurapu (1993) as

$$C_r = \frac{\Delta\sigma_3}{2}\sqrt{K_p} \quad (5)$$

K_p is the coefficient of passive earth pressure and is a function of the friction angle of the infill soil which is normally the base material. The angle of internal friction for geocell confined soil layer remains same as for unreinforced soil as concluded by Rajagopal et al. (1999). Knowing the equivalent Young's modulus and friction angle of the base soil and the corresponding cohesion, the effect of geocell in a pavement section can be evaluated based on mechanistic empirical design of pavements.

2.3 Model Considerations

A two dimensional (2D) axisymmetric analysis is adopted in this study and analysis is performed using FLAC version 5. (Fast Lagrangian Analysis of Continua). Soil is modelled as Mohr Coulomb model) and the asphalt concrete is modelled as an elastic model. The geocell-reinforced layer is also modelled using Mohr Coulomb model with the equivalent values of Young's modulus and shear strength properties calculated from composite model from equations given in the previous sections.

2.4 Load Considerations

It is assumed that load of one set of dual tires is transferred to the pavement surface through a contact pressure of a single tire and the load for the single tire is 40 kN. The tire contact pressure on the pavement is considered to be equal to the tire pressure, which is taken as 570 kPa. Consideration of the shape of the load surface as infinite long strip, plain strain model, leads to an overestimation of the results and as a circular surface leads to the realistic desired response. So the pavement is modelled as axisymmetric model and a circular surface loading of 570kPa with 150mm radius, this is equivalent to 40.3 kN load, is adopted for the present numerical analysis.

2.5 Boundary Conditions

Conventional kinematic boundary conditions are adopted, i.e., all the vertical boundaries are fixed in horizontal direction and free to move vertical direction of the model and the movement of the bottom of the model is fixed in both horizontal and vertical directions. The properties of the materials adopted in the analysis are given in Table 1.The thickness of the sand layer is chosen based on IRC guidelines.

Table 1 Properties of Asphalt Concrete, Base and Subgrade

Layer	**Asphalt-concrete**	**Base**	**Subgrade**
Material	Asphalt-concrete	Sand	Soft soil
Model	Elastic	Mohr Coulomb	Mohr Coulomb
Elastic Modulus M Pa	4134.69	75	8.25
Poisson's ratio	0.3	0.35	0.35
Unit weight kN/m^3	24	18	17
Cohesion kPa	-	8	20
Friction angle °	-	36	0
Dilation angle °	-	0	0
Thickness mm	50	250	2700

Two different locations of the geocell are adopted in the present study to understand the effect of the location of geocell on the behaviour of the pavement. In one case, the geocell is placed below AC layer and in the second case it is placed below base layer, as shown in Figure 2.

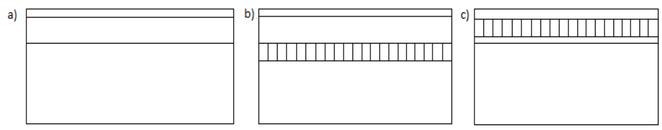

Figure 2 Locations of the geocell: a) unreinforced; b) below base layer; c) below AC layer

3.0 ANALYSIS RESULTS

The vertical surface deflection is plotted against the distance from the centre of load. In addition, the fatigue strain and rutting strain are evaluated at the bottom of AC layer and top of subgrade layer respectively below the centre line of the load. The effect of secant modulus of geocell material, effect of the thickness of geocell-reinforced layer, effect of aspect ratio and effect of type of subgrade are studied in the parametric study. The Young's modulus and shear strength parameters for geocell-reinforced soil layer corresponding to different sets of values of secant modulus, pocket size, thickness of geocell-reinforced layer and infill soil properties for the parametric study are calculated by using the composite model. The results evaluated for different models are shown and discussed in the following subsections.

3.1 Effect of geocell reinforcement at different locations

The geocell placed at two different locations, below base layer infilled with soft soil and below AC layer infilled with sand respectively. The secant modulus, pocket size and thickness of geocell-reinforced soil layer are taken as 500kN/m at 2.5% axial strain, 100 mm and 200 mm respectively for both the reinforced conditions.

For the geocell-reinforced pavement with geocell placed below base layer the extra confinement is 129.01 kPa. This leads to an extra cohesive strength as 64.51 kPa. So the shear strength parameters for geocell-reinforced layer are 84.51 kPa as cohesive strength and the angle of friction does not change in the presence of geocell. The Young's modulus of geocell-reinforced soil layer is 104.36 MPa. Similarly the Young's modulus and shear strength parameters for geocell-reinforced sand layer for geocell placed below AC layer can be calculated. The surface settlement-distance from the centre line plots obtained from numerical analysis for reinforced and unreinforced pavement with different locations of geocell are plotted in Figure 3.

As shown in Figure 3, the geocell reinforcement reduces the surface settlement of the pavement. The settlement reduction is more pronounced when the geocell placed near the loading i.e. when placed below the AC layer. The surface settlements at the centre of loading are 4.08 mm, 3.0 mm and 1.82 mm for unreinforced, reinforced with geocell placed below base layer and below AC layer respectively.

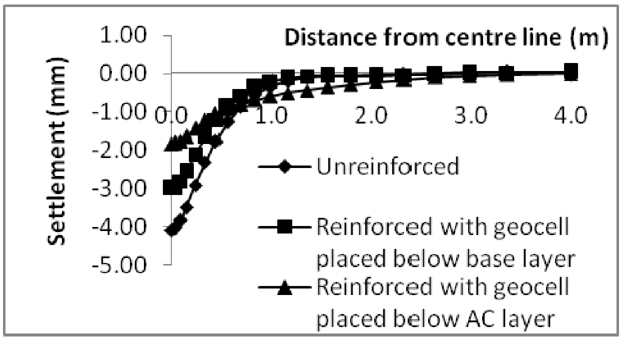

Figure 3 Surface settlement response for reinforced and unreinforced pavement

3.2 Effect of secant modulus of geocell material

The different values of secant modulus for geocell are adopted as 100, 200, 300, 400 and 500 kN/m respectively to understand the surface settlement response of pavement and fatigue and rutting strains. In all these cases the geocell is placed below AC layer and same size of geocell (i.e. D =100 mm, h=200 mm) with similar soil properties is modelled. The surface settlement-distance from the centre line curves from numerical analysis is presented in Figure 4.

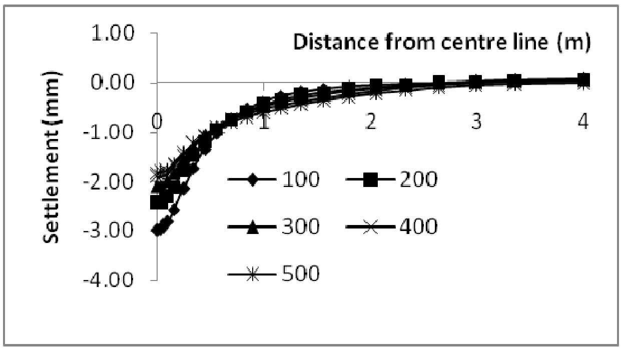

Figure 4 Surface settlement response for different values of secant modulus of geocell

The figure shows that the surface settlement get reduces as the secant modulus of geocell increases. This result is expected because geocell with higher secant modulus value provides higher extra confinement to the infill soil which leads to the higher modulus and cohesive strength to the infill soil, provided the geocell pocket size is the same. The settlement reductions for secant modulus 400 kN/m and 500 kN/m are almost same. The strains evaluated for different models are presented in Table 2. The results show that the reduction in fatigue and rutting strains increases with increase in the secant modulus of geocell material. But the rutting strains are almost same for secant modulus value of 300 kN/m and more. Hence, it can be concluded that geocells do not need to be made of very stiff material.

Table 2 Fatigue and rutting strains

S. No.	Secant modulus of geocell material, M' (kN/m)	Fatigue $\varepsilon_t^{max} \times 10^{-6}$	Rutting $\varepsilon_c^{max} \times 10^{-6}$
1	N/A	1610	-6850
2	100	950	-5440
3	200	640	-3800
4	300	430	-3290
5	400	270	-3210

3.3 Effect of the thickness of geocell-reinforced layer

The thickness of sand layer (i.e. base layer) is 250 mm, so the thickness of geocell-reinforced sand layers are taken as 100 mm, 150 mm and 200 mm respectively to understand the surface settlement of the pavement. In all these cases the geocell is placed below AC layer and same pocket size, secant modulus of geocell (i.e. D =200 mm, M'=500 kN/m) with similar soil properties are used. The surface settlement-distance from the centre line plots from numerical analysis is plotted together in Figure 5. The figure shows that the surface settlement reduces as the thickness of geocell-reinforced sand layer increases with pocket size of geocell, secant modulus of geocell and soil properties being the same. But the settlements are differentiable only near the loading position. Table 3 shows the reduction in the strains with increase in the thickness of the geocell-reinforced soil layer.

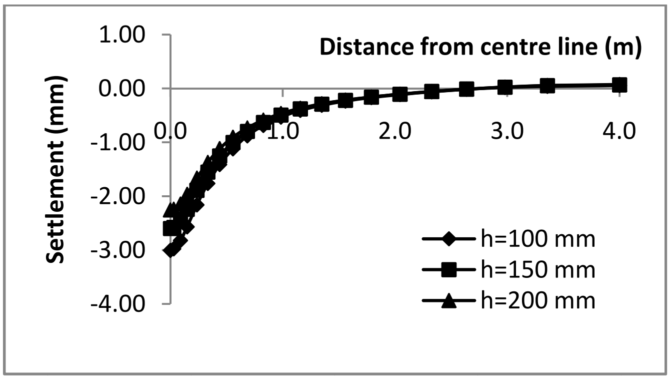

Figure 5 Variation of settlement as a function of thickness of geocell reinforced layer

Table 3 Fatigue and rutting strains

S. N.	Height of geocell layer, h (mm)	Fatigue $\varepsilon_t^{max} \times 10^{-6}$	Rutting $\varepsilon_c^{max} \times 10^{-6}$
1	N/A	1610	-6850
2	100	1050	-4370
3	150	760	-3900
4	200	540	-3370

3.4 Effect of aspect ratio

Different values of aspect ratio are achieved by varying the pocket size (i.e. diameter) of geocell for geocell-reinforced layer provided the height of geocell layer constant as 200 mm. The secant modulus of geocell is same for all the above numerical analysis and taken as 500 kN/m. The change in pocket size in geocell-reinforced layer is simulated in the numerical analysis by using the different values of elastic modulus and cohesion and is calculated using the composite model. The surface settlement-distance profiles from the centre line are presented in Figure 6.

It can be noted that surface settlement reduces as the aspect ratio increases, but this is insignificant for higher value of aspect ratio. The settlement values for aspect ratios 1.5 and 2 are same and this is comparable to the settlement for aspect ratio 1. This suggests that the aspect ratio 1 can be considered as the optimal value for the geocell layer. Table 4 shows that the reduction in fatigue and rutting strains increases with the increase in aspect ratio of the geocell material. But the reduction in rutting strain is almost same for aspect ratio 1, 1.5 and 2.0. Hence lower aspect ratios are not preferable and optimum ratio of 1 is desirable for better performance of pavement.

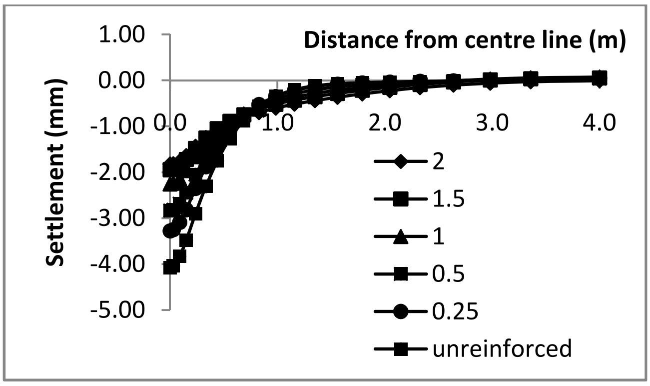

Figure 6 Surface settlement response for different values of aspect ratio of geocells

Table 4 Fatigue and rutting strains

Initial diameter of geocell, D (mm)	Height of geocell layer, h (mm)	Aspect ratio of geocell (h/D)	Fatigue $\varepsilon_t^{max} \times 10^{-6}$	Rutting $\varepsilon_c^{max} \times 10^{-6}$
N/A	N/A	N/A	1610	-6850
800	200	0.25	1120	-6060
400	200	0.5	860	-4850
200	200	1.0	540	-3370
133	200	1.5	300	-3250
100	200	2.0	160	-2890

3.5 Effect of type of subgrade

The Young's modulus and shear strength parameters of the subgrade increased to twice (i.e. E=16.5 MPa and c_u =40 kPa) the present value to understand the behaviour of the pavement for relatively stiffer subgrade. The surface settlement-distance from the centre line curves from numerical analysis are presented in Figure 7.

The results show that the settlement of both reinforced and unreinforced pavement, for stiff subgrade, decreased and this is expected. It is also noticed that the settlement for geocell-reinforced sand layer over soft subgrade is lower that the settlement for unreinforced sand layer over relatively stiff subgrade. This means the geocell-reinforced flexible pavement with soft subgrade can perform better than the unreinforced flexible pavement with stiff subgrade.

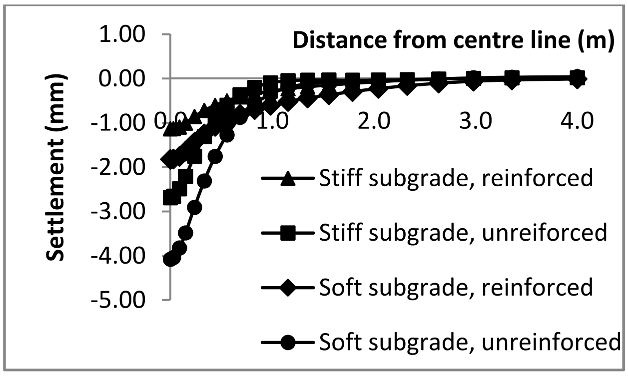

Figure 7 Surface settlement response for different type of subgrade

4. CONCLUSIONS

The following conclusions are made based on the work reported in this study. An analytical equation is suggested for the composite modulus of the geocell confined soil. Using the composite modulus values, a parametric study is conducted to examine the influence of secant modulus of geocell material, effect of the thickness of geocell-reinforced layer, effect of aspect ratio and effect of type of subgrade using numerical analysis. The results show that provision of geocell in the granular sub base helps in pavement performance expressed in terms of settlements, fatigue and rutting strains. Thickness of the geocell confined soil as well as the aspect ratio of geocell, type of the soil play a significant role in pavement performance.

5. ACKNOWLEDGEMENTS

The work reported in this paper is a part of the research project on the GUIDELINES FOR THE USE OF GEO-CELLS IN FLEXIBLE PAVEMENTS sponsored by the Department of Science and Technology, New Delhi. Their financial support in the project is gratefully acknowledged.

6. REFERENCES

Bathurst, R. J., and Karpurapu, R. (1993) "Large-scale triaxial compression testing of geocell-reinforced granular soils", Geotech. Test. J., 16, pp296–303.

Bush, D. I., Jenner, C. G., and Bassett, R. H. (1990) "The design and construction of geocell foundation mattress supporting embankments over soft ground", Geotext.Geomembr., 9, pp83–98.

Cowland, J. W., and Wong, S. C. K. (1993) "Performance of a road embankment on soft clay supported on a geocell mattress foundation", Geotext.Geomembr., 12, pp687–705.

FLAC (version 5.0) – Fast Lagrangian analysis of continua, Itasca Consulting Group, Inc., Minneapolis, Minnesota, USA, 2005.

Henkel, D. J., and Gilbert, G. D. (1952) "The effect of the rubber membrane on the measured triaxial compression strength of clay samples", Geotechnique, 3(1), pp20–29.

IRC: 37-2001 "Guidelines for the design of flexible pavement", Indian Road Congress, New Delhi.

Madhavi Latha, G., Dash Sujit Kumar, Rajagopal, K. (2009) "Numerical simulation of the behaviour of geocell reinforced sand in foundations", International Journal of Geomechanics, ASCE, Vol. 9, No. 4, pp143-152.

Mitchell, J. K., Kao, T. C., and Kavazanjian, E. (1979) "Analysis of grid cell reinforced pavement bases", Technical Rep. GL-79–8, U.S. Army Engineer Waterways Experiment Station, Vicksburg.

Rajagopal, K., Krishnaswamy, N. R., and Madhavi Latha, G. (1999) "Behavior of sand confined in single and multiple geocells", Geotext.Geomembr., 17, pp171–184.

Sanat K. P, Jie Han, Dov Leshchinsky, Robert L. Parsons and Izhar Halahmic (2010) Investigation of factors influencing behavior of single geocell-reinforced bases under static loading Geotextiles and Geomembranes Volume 28 (6,)570–578.

Sivakumar Babu G L and Pawan Kumar (2012) An approach for evaluation of Geocells in flexible pavements, Journal of Indian Roads Congress, Paper No 578, 159-168.

Webster, S.L. & Watkins J.E. (1977), Investigation of Construction Techniques for Tactical Bridge Approach Roads Across Soft Ground. Soils and Pavements Laboratory, U.S. Army Corps of Engineers Waterways Experiment Station, Vicksburg, MS, Technical Report S771, September 1977.

Yang Xiaoming, Jie Han, Robert L. Parsons, Dov Leshchinsky (2010) “Three-dimensional numerical modelling of single geocell reinforced sand”, Front. Archit. Civ. Eng. China 2010, 4(2), pp233–240.